Scientific Research and Essays Vol. 6(20), pp. 4354-4368, 19 September, 2011
Available online at http://www.academicjournals.org/SRE
DOI: 10.5897/SRE10.876
ISSN 1992-2248 ©2011 Academic Journals

Full Length Research Paper

ISO 9164 heat loss in roof-wall sections

Abdurrahman GÜNER[1], Şükran DİLMAÇ[2] and M. Timur CİHAN[3]*

[1]Department of Civil Engineering, Faculty of Engineering,Istanbul University, Istanbul, Turkey.
[2]Environment Energy Efficiency and Quality Committee Charter, CEVKAK, Basaksehir,Istanbul, Turkey.
[3]Department of Civil Engineering, Corlu Faculty of Engineering, Namik Kemal University, Tekirdag-Corlu, Turkey.

Accepted 22 August, 2011

In the simple ISO 9164 calculation procedure for transmission heat loss coefficient, H_T, it is unclear, and undefined for floor or roof-wall sections, how the parameters in the equations will be calculated. In this paper, a method is proposed for the calculation of ISO 9164 parameters for roof-wall sections. The results obtained by the proposed method for typical roof sections are compared with those obtained by the EN 832/EN 13789/EN ISO 14683 methods and with the L^{2D} values from 2D analysis. A comparison of the floor and roof behaviour is realized using the results of the present and the previous works of the authors. The H_T values obtained by the proposed model using the sum of q_y through the beam are harmonised with the L^{2D} for floors, which are significantly different from the L^{2D} for roofs with parapet. The results indicate that the L^{2D} values cited in EN 10211-1 are sensitive to the 2D heat flows for floor sections. However, the L^{2D} is not sufficiently sensitive to heat flow from the beam to the parapet and the interactions between the zones within the beam section, whereas the proposed method is more sensitive to the 2D heat flows.

Key words: Thermal bridges, 2D thermal analysis, heat loss, heat transmittance coefficient, thermal analysis.

INTRODUCTION

Thermal bridges with limited area but quite high thermal transmittance than average cause significant decrease in the thermal performance of buildings. There are numerous researches on the thermal behaviour of these regions. One of the earliest thoroughly investigates the effect of the position and dimension of insulating layer on the inside surface temperature, and the difference between the measured and calculated values by 1D analysis (Brown et al., 1963). A significant portion of the researches are on the development and improvement of comprehensive commercial or non-commercial software programs based on finite difference / finite element / finite volume methods and with progressively higher accuracy, repeatability, user friendliness and flexibility (Larbi, 2005; Mao et al.,1997; Matrosov et al.,1989; Salgon et al.,1987; Al-Anzi et al., 2004; Al-Sanea, 2003; Van Schijindel, 2003;Malas et al.,1992; Hassid,1990; Hassid,1989;Yahia et al.,1999; Fukuyo, 2003). Some of the others are on the transfer of the results obtained by these software programs analysing single certain component into other software programs designed to analyse the thermal performance of a whole building (Zhai et al., 2002; Kosny et al., 2002; Deque et al., 2001; Lefebvre, 1997). The results are compared with the experimental results or with those obtained by using default values given in tables. In those works, different quantities are calculated by using equations different from those in the standards (ISO 9164, EN 832, etc.). Therefore, the results and information given in these researches were considered not suitable for use in the calculation and comparison of heat loss according to the above-mentioned standards.

As mentioned earlier, international standards on calculation of space heating requirements for residential buildings are ISO 9164 and EN 832 (Anon ISO 9164,

*Corresponding author. E-mail: timurcihan@gmail.com, mehmetcihan@nku.edu.tr. Tel:+ 90 282 652 9475. Fax:+90 282 652 9372.

1989; Anon EN 832, 2000). Although they are based on similar principles, there are significant differences between the corresponding calculation procedures of transmission heat loss coefficient, H_T, especially in the evaluation of thermal bridges.

Calculation procedure defined in ISO 9164 is simpler. But how the parameters ξ and U_ℓ should be calculated is not defined. So, it is impossible to calculate and compare thermal performance of buildings according to this standard in the present case. The aim of this research is to make serviceable the ISO 9164 in which the calculation procedure is simpler than EN 832. In Ref. (Dilmac et al., 2007), a method is proposed for the calculation of the parameters for floor-wall intersections. In this paper, the same method is applied to roof-wall (terrace-wall) intersections. To evaluate the method, the results obtained by the proposed method for typical roof sections (Table 1) are compared with the results obtained by the methods stated in EN 832/EN 13789 (Anon EN ISO 13789, 1999 EN ISO 14683: Anon ISO 14683, 1999) and the L^{2D} values obtained from 2D analysis. In order to make this comparison, H_T values are calculated for 1.00 m section thickness using the equation "$\sum A \cdot U + \sum \ell \cdot U_\ell$" given in ISO 9164, including the parameters determined by the proposed method, for the sections with two different lengths. The lengths of walls and reinforced concrete floor slab from outside corner, in the first one are equal to 0.80 m, and, in the second one, equal to 1.00 m. The second one can be considered to be equivalent to L^{2D} given in EN 13789, EN ISO 14683 and ISO EN 10211-1 (Anon EN ISO 10211-1,1996).

H_T values obtained by the proposed model by using the sum of q_y through the beam are harmonised with the L^{2D} for floors. But these are significantly different from the L^{2D} for roofs with parapet. In this work, these differences are also analysed. In order to assess the sensitivity of the method to the 2D heat flow, each value is compared with the value calculated by 1D analysis. In addition, H_T values are calculated again according to the proposed method, but by using the average volume heat flux density through the beam, and are compared with the L^{2D} values for roofs, so as to see if the method is sensitive to the interaction between the zones within the beam section. The results obtained indicate that L^{2D} values cited in EN 10211-1 are sensitive to the 2D heat flows for floor sections, but are not sensitive enough for the sections of roof with parapet. The L^{2D} is not sufficiently sensitive to heat flow from the beam to the parapet and the interaction between the zones within the beam section whereas the proposed method is more sensitive to the 2D heat flows through the roof sections with parapet.

PROPOSAL FOR THE CALCULATION OF THE 2D PARAMETERS

Methods given in the standards (ISO 9164 and EN 832) are explained in Ref. (Dilmac et al., 2007). The proposed method is different from that given in Ref. (Dilmac et al., 2007) and is explained as follows.

A thorough analytical examination of the heat fluxes through the sections forming the beam+roof slab, could be suitably considered as beams only, on condition that heat flux in the beam is determined for at least three separate regions (Figure 1). Depth of beam (for example, h_{beam}= 0.60 m in this work) is divided into three regions. Upper region is defined by the flange height of the floor slab (for example, h_u= 0.15 m), whereas the middle region by the segment of 0.25 m height below the bottom surface of slab, and the lower region by the segment of 0.20 m height from the base of the beam (Figure 1). In the upper region, corresponding to the slab level, extra heat flux in the *y* direction due to the corner effect is also taken into consideration. In this part, lateral heat flux from the beam to the parapet wall in the y direction (upwards) also exists. The lower part is a region in which lateral heat flux from the wall to the beam in the y direction (upwards) takes place. In the middle region, generally, the heat flux in the y direction is minimal. The magnitudes of these effects depend on the existence and the place of heat insulation layer in the section.

The average volume heat flux densities in the x and y directions, and the resultant average volume heat flux density together with the angle it makes with the x direction are obtained by using QuickField for each region (Figure 1). Then, arithmetic mean q_x is calculated by Equation (1) using the q_x values obtained by 2D analysis for each region:

$$q_x = \frac{0.15 \cdot q_{x\,\text{upper}} + 0.25 \cdot q_{x\,\text{middle}} + 0.20 \cdot q_{x\,\text{lower}}}{0.60} \quad (1)$$

This "q_x" should satisfy the following 1D equation:

$$q_x = \Lambda \cdot (T_{is} - T_{os}) \quad (2)$$

T_{is} and T_{os} are determined as the average values calculated along the line at the inside surface (continuing across the thickness of the slab) and outside surface of the beam by using the software. Then, the value of Λ is obtained from Equation (2). The notation "Λ_{q_x}" is used to indicate that it is obtained using q_x from 2D analysis (Equation 1). Equivalent thicknesses of layers to yield the "Λ_{q_x}" value are determined by using Equations 3, 4, 5 and 6.

Calculations are made for two cases of each section, with plaster and without plaster, in order to examine the difference. If the differences come out to be insignificant, plaster layers can be ignored in calculation for reducing the number of operations.

Equations for the sections with no insulation are:

Plaster excluded: $$\left(\frac{1}{\Lambda_{q_x}}\right) \cdot \lambda_c = d_{e,c}\,, \quad (3)$$

Plaster included: $$\left(\frac{1}{\Lambda_{q_x}} - \frac{d_{ip}}{\lambda_{ip}} - \frac{d_{op}}{\lambda_{op}}\right) \cdot \lambda_c = d_{e,c} \quad (4)$$

The value for $d_{e,c}$ is around 0.30 m. This can be taken to mean that a modification of the classical equation for U_{TB} ($U = 1/(1/\alpha_i + \sum(d/\lambda) + 1/\alpha_o)$) is not needed (Table 2).

Computations are performed using the following equations for sections with insulation:

Table 1. Roof sections examined.

Sections[a]	Properties of sections	Outer plaster	Inner plaster	Brick wall	Floor slab	Width of beam	Height of beam	Alum	Ceiling plaster	Reinforce concrete	insulation
UI1	Thicknesses[c]	0.025	0.015	0.200	0.150	0.300	0.600	0.030	0.015	-	-
	Thermal conductivities[d]	0.87	0.87	0.45	-	-	-	1.4	0.87	2.1	-
UI2	Thicknesses	0.025	0.015	0.200	0.150	0.300	0.600	0.030	0.015	-	-
	Thermal conductivities	0.87	0.70	0.45	-	-	-	1.4		2.1	-
EI1	Thicknesses	0.008	0.015	0.200	0.150	0.300	0.600	0.030	0.015	-	0.05
	Thermal conductivities	0.80	0.87	0.45	-	-	-	1.4		2.1	0.04
EI2	Thicknesses	0.008	0.015	0.200	0.150	0.300	0.600	0.030	0.015	-	0.050
	Thermal conductivities	0.80	0.87	0.45	-	-	-	1.4		2.1	0.04
II1	Thicknesses	0.025	0.010	0.200	0.150	0.300	0.600	0.030	0.015	-	0.05
	Thermal conductivities	0.87	0.70	0.45	-	-	-	1.4		2.1	0.04
II2	Thicknesses	0.025	0.010	0.200	0.150	0.300	0.600	0.030	0.015	-	0.05
	Thermal conductivities	0.87	0.70	0.45	-	-	-	1.4		2.1	0.04
CWI1	Thicknesses	0.025	0.015	2*0.10	0.150	0.300	0.600	0.030	0.015	-	0.05
	Thermal conductivities	0.87	0.87	0.45	-	-	-	1.4		2.1	0.04
CWI2	Thicknesses	0.025	0.015	2*0.10	0.150	0.300	0.600	0.030	0.015	-	0.05
	Thermal conductivities	0.87	0.87	0.45	-	-	-	1.4		2.1	0.04
CWI3[b]	Thicknesses	0.025	0.015	2*0.10	0.150	0.300	0.600	0.030	0.015	-	0.05
	Thermal conductivities	0.87	0.87	0.45	-	-	-	1.4		2.1	0.04

[a]Height of parapet is 0.50 m. [b]Thickness of internal plaster on the beam is 0.010 m. [c and d] The units of thicknesses and thermal conductivities are m and W/(m·K), respectively.

Without plaster: $$\left(\frac{1}{\Lambda_{q_x}}-\frac{d_c}{\lambda_c}\right)\cdot\lambda_{ins.}=d_{e,ins.} \quad (5)$$

With plaster: $$\left(\frac{1}{\Lambda_{q_x}}-\frac{d_c}{\lambda_c}-\frac{d_{ip}}{\lambda_{ip}}-\frac{d_{op}}{\lambda_{op}}\right)\cdot\lambda_{ins.}=d_{e,ins.} \quad (6)$$

In general, the equivalent thickness of an insulation layer, $d_{e,ins.}$, calculated by Equations 5 and 6 is less than the actual thickness, varying with the position of insulation layer in the section. These results show that significant variations will occur on the heat loss when insulation is

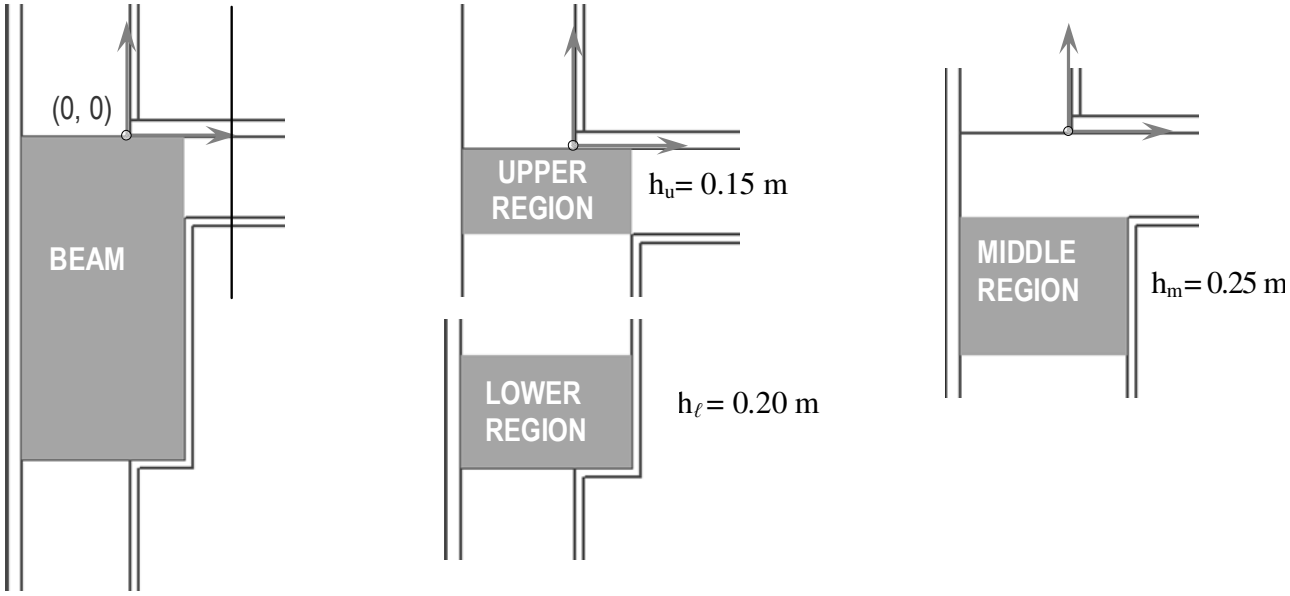

			BEAM (WHOLE)	UPPER	MIDDLE	LOWER
q_{ax}	(W/m^2)	=	- 28.7	- 14.8	- 29.4	- 38.2
q_{ay}	(W/m^2)	=	13.3	17.8	13.3	10.0
$q_{average}$	(W/m^2)	=	31.6	23.1	32.2	39.5
φ	(Degree)	=	155.1	129.8	155.6	165.4

φ is the angle between $q_{average}$ and x axis, (-) sign for q_x indicates a heat flux from right to left and (-) sign for q_y indicates a downward heat flux.

Figure 1. Example of heat flux calculations for the regions in a web beam.

applied. Consequently, thermal resistance of the section should be changed so as to meet extra heat loss, in order to represent actual situation (2D analysis results). For this purpose, the insulation thickness obtained by Equation 5 or 6 is divided by actual insulation thickness, and actual insulation thickness in the U_{TB} equation is multiplied by this ratio. The results are presented in Table 2.

On the other hand, the values of q_y are used for calculating "ξ" representing lateral heat loss. The computational procedure used is as follows:

Firstly, lateral heat loss is determined by summing the q_y of each region (Figure 1) (Equation 7).

$$q_y = q_{y\,upper} + q_{y\,middle} + q_{y\,lower} \quad (7)$$

As noted in Ref. (Dilmac et al., 2007), ξ may be interpreted as representing the heat transferred in the *y* direction through the area of width d_{beam} and length 1 m. It must be in W/(m·K) units according to Equation (2) in Ref. (Dilmac et al., 2007). In this case, ξ can be calculated by using the Equations 8, 9, 10 and 11 in which the known values of d_{beam}, d_{ins}, d_{ip}, d_{op} and computed values of q_y, T_{is} and T_{os} are used.

For sections with no insulation:

Plaster excluded: $$\xi = \frac{q_y \cdot d_{beam} \cdot 1.00}{T_{is} - T_{os}} \quad (8)$$

Plaster included: $$\xi = \frac{q_y \cdot (d_{beam} + d_{ip} + d_{op}) \cdot 1.00}{T_{is} - T_{os}} \quad (9)$$

For sections with insulation:

Plaster excluded: $$\xi = \frac{q_y \cdot (d_{beam} + d_{ins.}) \cdot 1.00}{T_{is} - T_{os}} \quad (10)$$

Plaster included: $$\xi = \frac{q_y \cdot (d_{beam} + d_{ins.} + d_{ip} + d_{op}) \cdot 1.00}{T_{is} - T_{os}} \quad (11)$$

Computations were carried out using Excel worksheets. Table 2 shows the numerical results' columns only. The other columns containing the equations and the values used in the computations are not shown.

RESULTS AND DISCUSSION

Nine typical roof sections are examined (Table 1). In the sections studied, the origin, the point (0, 0), is shown in Figure 2. The roof slab extends 0.80 m from this point to the inside in the model sections analysed (Series A). The

Table 2. Variations of the parameters depending on the positions of the insulation layers.

Sections		$d_{calc.}/d_{real}$	U_{TB}, W/(m²·K)		ξ, W/(m·K)		U_{ℓ}, W/(m·K)	
			Equation	Value	Equation	Value	Equation	Value
UI1	Plaster excluded	1.001	$\frac{1}{\frac{1}{\alpha_i}+\frac{1}{\alpha_o}+\frac{d_{TB}}{\lambda_{TB}}}$	3.20	$\frac{q_y \cdot d_{TB} \cdot 1}{T_{is}-T_{os}}$	3.01	$(b \cdot U_{TB})+\xi$	4.93
	Plaster included	0.984	$\frac{1}{\frac{1}{\alpha_i}+\frac{1}{\alpha_o}+\frac{d_{TB}}{\lambda_{TB}}+\frac{d_{op}}{\lambda_{op}}+\frac{d_{ip}}{\lambda_{ip}}}$	2.79	$\frac{q_y \cdot (d_{TB}+d_{op}+d_{ip}) \cdot 1}{T_{is}-T_{os}}$	2.50	$(b \cdot U_{TB})+\xi$	4.17
UI2	Plaster excluded	1.003	$\frac{1}{\frac{1}{\alpha_i}+\frac{1}{\alpha_o}+\frac{d_{TB}}{\lambda_{TB}}}$	3.20	$\frac{q_y \cdot (d_{TB}+d_{ins.}) \cdot 1}{T_{is}-T_{os}}$	3.28	$(b \cdot U_{TB})+\xi$	5.20
	Plaster included	0.966	$\frac{1}{\frac{1}{\alpha_i}+\frac{1}{\alpha_o}+\frac{d_{TB}}{\lambda_{TB}}+\frac{d_{op}}{\lambda_{op}}+\frac{d_{ip}}{\lambda_{ip}}}$	2.79	$\frac{q_y \cdot (d_{TB}+d_{ins.}+d_{op}+d_{ip}) \cdot 1}{T_{is}-T_{os}}$	2.76	$(b \cdot U_{TB})+\xi$	4.43
EI1	Plaster excluded	0.580	$\frac{1}{\frac{1}{\alpha_i}+\frac{1}{\alpha_o}+\frac{0.6 \cdot d_{ins.}}{\lambda_{ins.}}+\frac{d_{TB}}{\lambda_{TB}}}$	0.94	$\frac{q_y \cdot (d_{TB}+d_{ins.}) \cdot 1}{T_{is}-T_{os}}$	2.39	$(b \cdot U_{TB})+\xi$	2.96
	Plaster included	0.568	$\frac{1}{\frac{1}{\alpha_i}+\frac{1}{\alpha_o}+\frac{0.55 \cdot d_{ins.}}{\lambda_{ins.}}+\frac{d_{TB}}{\lambda_{TB}}+\frac{d_{op}}{\lambda_{op}}+\frac{d_{ip}}{\lambda_{ip}}}$	0.97	$\frac{q_y \cdot (d_{TB}+d_{ins.}+d_{op}+d_{ip}) \cdot 1}{T_{is}-T_{os}}$	2.45	$(b \cdot U_{TB})+\xi$	3.04
EI2	Plaster excluded	0.611	$\frac{1}{\frac{1}{\alpha_i}+\frac{1}{\alpha_o}+\frac{0.6 \cdot d_{ins.}}{\lambda_{ins.}}+\frac{d_{TB}}{\lambda_{TB}}}$	0.94	$\frac{q_y \cdot (d_{TB}+d_{ins.}) \cdot 1}{T_{is}-T_{os}}$	0.92	$(b \cdot U_{TB})+\xi$	1.49
	plaster included	0.599	$\frac{1}{\frac{1}{\alpha_i}+\frac{1}{\alpha_o}+\frac{0.6 \cdot d_{ins.}}{\lambda_{ins.}}+\frac{d_{TB}}{\lambda_{TB}}+\frac{d_{op}}{\lambda_{op}}+\frac{d_{ip}}{\lambda_{ip}}}$	0.92	$\frac{q_y \cdot (d_{TB}+d_{ins.}+d_{op}+d_{ip}) \cdot 1}{T_{is}-T_{os}}$	0.94	$(b \cdot U_{TB})+\xi$	1.49
II1	Plaster excluded	0.444	$\frac{1}{\frac{1}{\alpha_i}+\frac{1}{\alpha_o}+\frac{0.45 \cdot d_{ins.}}{\lambda_{ins.}}+\frac{d_{TB}}{\lambda_{TB}}}$	1.14	$\frac{q_y \cdot (d_{TB}+d_{ins.}) \cdot 1}{T_{is}-T_{os}}$	0.51	$(b \cdot U_{TB})+\xi$	1.19
	Plaster included	0.440	$\frac{1}{\frac{1}{\alpha_i}+\frac{1}{\alpha_o}+\frac{0.45 \cdot d_{ins.}}{\lambda_{ins.}}+\frac{d_{TB}}{\lambda_{TB}}+\frac{d_{op}}{\lambda_{op}}+\frac{d_{ip}}{\lambda_{ip}}}$	1.09	$\frac{q_y \cdot (d_{TB}+d_{ins.}+d_{op}+d_{ip}) \cdot 1}{T_{is}-T_{os}}$	0.57	$(b \cdot U_{TB})+\xi$	1.22
II2	Plaster excluded	0.269	$\frac{1}{\frac{1}{\alpha_i}+\frac{1}{\alpha_o}+\frac{0.25 \cdot d_{ins.}}{\lambda_{ins.}}+\frac{d_{TB}}{\lambda_{TB}}}$	1.60	$\frac{q_y \cdot (d_{TB}+d_{ins.}) \cdot 1}{T_{is}-T_{os}}$	0.27	$(b \cdot U_{TB})+\xi$	1.23
	plaster included	0.265	$\frac{1}{\frac{1}{\alpha_i}+\frac{1}{\alpha_o}+\frac{0.25 \cdot d_{ins.}}{\lambda_{ins.}}+\frac{d_{TB}}{\lambda_{TB}}+\frac{d_{op}}{\lambda_{op}}+\frac{d_{ip}}{\lambda_{ip}}}$	1.50	$\frac{q_y \cdot (d_{TB}+d_{ins.}+d_{op}+d_{ip}) \cdot 1}{T_{is}-T_{os}}$	0.25	$(b \cdot U_{TB})+\xi$	1.15
CWI1	Plaster excluded	0.982	$\frac{1}{\frac{1}{\alpha_i}+\frac{1}{\alpha_o}+\frac{d_{TB}}{\lambda_{TB}}}$	3.20	$\frac{q_y \cdot d_{TB} \cdot 1}{T_{is}-T_{os}}$	2.83	$(b \cdot U_{TB})+\xi$	4.75

Table 2. Contnd

	Plaster included	0.967	$\frac{1}{\frac{1}{\alpha_i}+\frac{1}{\alpha_o}+\frac{d_{TB}}{\lambda_{TB}}+\frac{d_{op}}{\lambda_{op}}+\frac{d_{ip}}{\lambda_{ip}}}$	2.79	$\frac{q_y\cdot(d_{TB}+d_{op}+d_{ip})\cdot 1}{T_{is}-T_{os}}$	2.34	$(b\cdot U_{TB})+\xi$	4.01
CWI2	Plaster excluded	1.001	$\frac{1}{\frac{1}{\alpha_i}+\frac{1}{\alpha_o}+\frac{d_{TB}}{\lambda_{TB}}}$	3.20	$\frac{q_y\cdot d_{TB}\cdot 1}{T_{is}-T_{os}}$	1.12	$(b\cdot U_{TB})+\xi$	3.04
	Plaster included	0.977	$\frac{1}{\frac{1}{\alpha_i}+\frac{1}{\alpha_o}+\frac{d_{TB}}{\lambda_{TB}}+\frac{d_{op}}{\lambda_{op}}+\frac{d_{ip}}{\lambda_{ip}}}$	2.79	$\frac{q_y\cdot(d_{TB}+d_{op}+d_{ip})\cdot 1}{T_{is}-T_{os}}$	0.93	$(b\cdot U_{TB})+\xi$	2.61
	Plaster excluded	0.176	$\frac{1}{\frac{1}{\alpha_i}+\frac{1}{\alpha_o}+\frac{0.15\cdot d_{ins.}}{\lambda_{ins.}}+\frac{d_{TB}}{\lambda_{TB}}}$	2.00	$\frac{q_y\cdot(d_{TB}+d_{ins.})\cdot 1}{T_{is}-T_{os}}$	0.56	$(b\cdot U_{TB})+\xi$	1.76
CWI3	plaster included	0.173	$\frac{1}{\frac{1}{\alpha_i}+\frac{1}{\alpha_o}+\frac{0.15\cdot d_{ins}}{\lambda_{ins}}+\frac{d_{TB}}{\lambda_{TB}}+\frac{d_{op}}{\lambda_{op}}+\frac{d_{ip}}{\lambda_{ip}}}$	1.85	$\frac{q_y\cdot(d_{TB}+d_{ins.}+d_{op}+d_{ip})\cdot 1}{T_{is}-T_{os}}$	0.54	$(b\cdot U_{TB})+\xi$	1.65

lengths of wall are also 0.80 m whereas the length of parapet is 0.50 m. Numbers of nodes in the finite element model are around 200 (182 to 202) (Dilmac et al., 2004). Properties of sections and network used in the analyses by the QuickField 5.1 program are shown in Table 1 and Figure 2, respectively. The 2D heat flux vectors and isotherms in the sections can be seen in Figure 2. In Table 2, the equations proposed for calculating U_{TB} and ξ by the proposed method are shown together with the corresponding numerical values obtained and the calculated U_ℓ values for the sections. The table also shows the results for the "plaster included" and "plaster excluded" cases.

Differences between the values for plaster excluded and included cases are significant, and from this point on, computations are made for the real case of plaster included only. To assess the reliability/accuracy of the magnitude of the results obtained by the proposed method, firstly, the parameters were calculated by this method and by the standard methods for the sections with two different lengths. One of them is named Series A, and described earlier. In the other, according to EN 10211, the lengths of walls and reinforced concrete (r.c.) roof slab from inside corner (the point (0.10, -0.15)) equal to 1.00 m (named Series B). Thus, it would also be possible to see the effect of the section lengths on the results which are given in Table 3 for comparison. All calculations were carried out for 1.00 m widths of the sections, hence, the units are W/(m·K) for both of H_T and L^{2D} values in the tables. H_T values calculated for the sections with 1.00 m lengths can be considered to be equivalent to L^{2D} given in EN ISO 14683 and EN 10211. Error analyses of the results obtained by the Quick Field program are shown in Table 4.

The numerical values in Table 3 show that the results obtained by the proposed method (H_T) for roofs are quite different from the results obtained by the EN ISO 14683 method (ψ and L^{2D}) and 2D analyses (L^{2D} values) performed by the QuickField program. Generally, the results obtained by the EN ISO 14683 method are less than those of the others as expected, because the sections in the standard have no web beams, so the effects of thermal bridges are less pronounced than the others.

In Figure 3, calculated quantities involving the H_T and L^{2D} values are shown. In the graphs on the right side (Figure 3e to 3g), the quantities are classified according to the section types (existence and place of insulation) while those on the left side (Figure 3a to 3d), the quantities are positioned in descending or ascending order. It is worth noting that the proposed method always gives significantly higher values for (H_T) than the other (L^{2D}). In Figure 3a and 3e, the curves of the H_T and L^{2D} values are shown. As expected, H_T and L^{2D} values are getting smaller and coming closer together if the roof has insulation, as in II2, EI2, CWI3, CWI2 and II1 in which 2D heat flow is less effective throughout the beam section, and/or the length of the heat flow vectors are smaller than the others (Figure 2). The higher differences between the H_T and L^{2D} values are seen at EI1, CWI1, UI1, and UI2 in which sections there is no roof insulation, and 2D heat flow throughout the beam section is clearly visible (Figures 2 and 3a and e).

The ratios of (L^{2D}/ H_T) have a slightly different trend (Figure 3b and 3f). (EI1 and EI2), (UI1 and UI2) and (CWI1) form a group and their L^{2D} values are about 70% of their H_T values obtained by the proposed method. As from CWI2, the ratios are significantly higher up to about

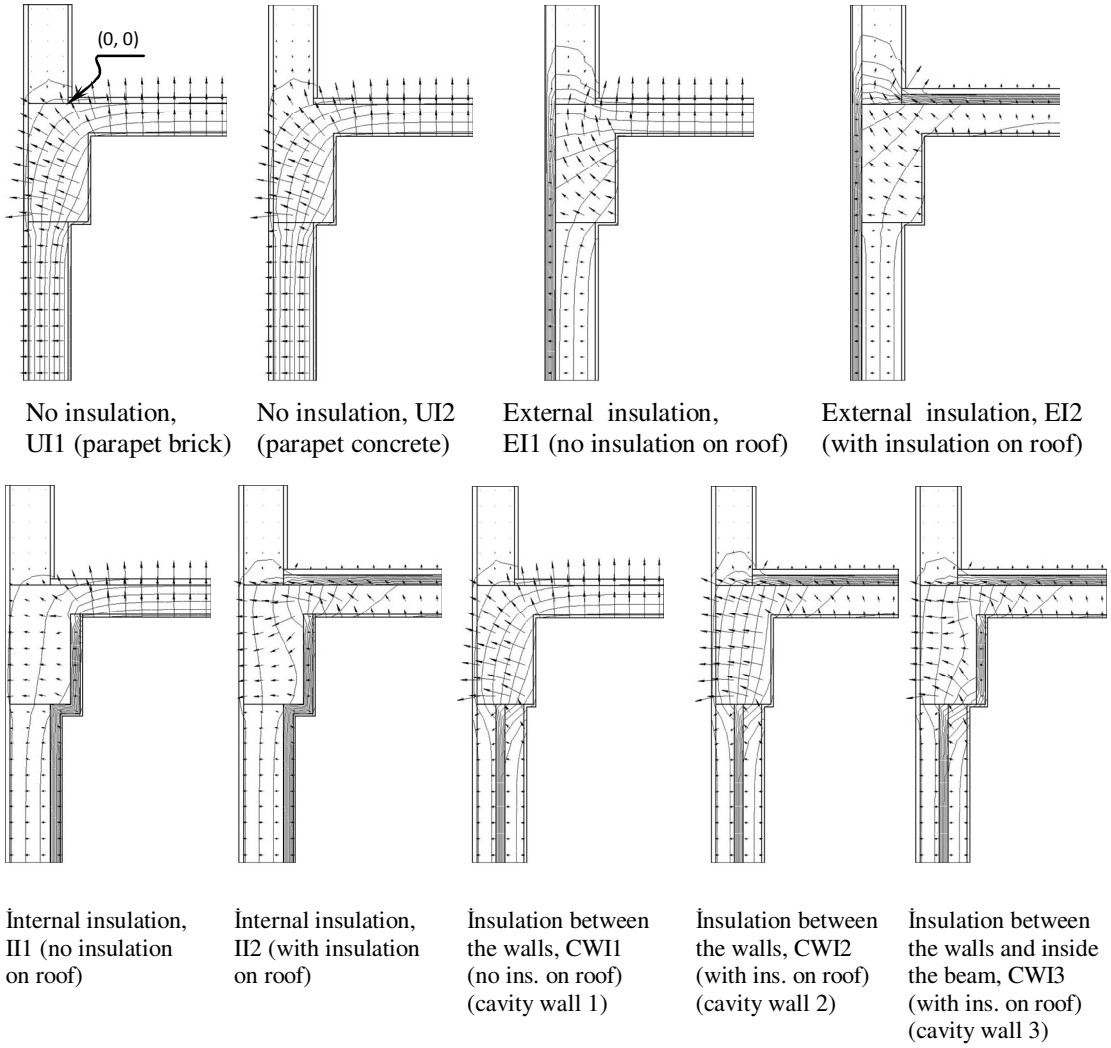

II1, II2, CWI2, CWI3, EI2 in which sections there are roof insulation except II1, 2D heat flow is less effective throughout the beam section, and/or the lengths of the heat flow vectors are smaller than the others.

UI2, UI1, CWI1, EI1 in which sections there are not roof insulation, and 2D heat flow throughout the beam section is clear.

Figure 2. Isotherms and heat flux vectors in the sections for T =20 C and T =8 C [Dilmac et al., 2004].

90%, CWI2, CWI3, II1 and II2 forming the other group. The values for the two dimensions examined (section Series A and B) are generally different but close up for EI2 and CWI2.

In calculation of H_T by the proposed method, q_y is determined by summing each absolute value of q_y of each region of beam (Figure 1). So this q_y defines the heat transfers (thermal interaction) in the beam, and it is more sensitive to the 2D heat flow throughout the beam caused by insulation type than L^{2D}. To assess which of the two is more accurate and closer to the real value, Table 5 is prepared. In this table, each value is compared with the value calculated by 1D analysis. In the 1D analysis, two approaches are used. In the first one, the upper region of the beam (Figure 1) is neglected. Hence, the lengths of roof slab, beam (≡h) and wall (that is, heat lost surface length) are 0.685 , 0.45 and 0.80 m, respectively, for sections of Series A, while those are 1.00 , 0.45 and 1.00 m for sections of Series B. In the second one, the upper region of the beam is supposed to be in contact with the indoor temperature. So, the lengths of roof, beam (≡h) and wall (that is, heat lost surface length) are 0.685 , 0.60 and 0.80 m, respectively, for sections of Series A, while those are 1.00 , 0.60 and 1.00 m for section of Series B. It is clear that real heat flow and the difference from 1D analysis will be relatively higher in the

Table 3. Comparison of the parameters calculated by the proposed method with those by the standard methods.

Section types	According to the proposed method							Default values given in EN ISO 14683[a]		According to the 2D analysis results (by QuickField)		$H_T - L^{2D}$	
	U_{TB} W/(m²·K)	ξ W/(m·K)	U_l W/(m·K)	U_{wall} W/(m²·K)	U_{roof} W/(m²·K)	H_T[b] W/(m·K)	H_T[c] W/(m·K)	ψ_{oi} W/(m·K)	L^{2D} W/(m·K)	L^{2D} [d] W/(m·K)	L^{2D} [e] W/(m·K)	[b] - [d] W/(m·K)	[c] - [e] W/(m·K)
UI1	2.79	2.50	4.17	1.51	3.57	7.82	9.25	-	-	5.26	6.64	2.56	2.61
UI2	2.79	2.76	4.43	1.51	3.57	8.08	9.51	-	-	5.30	6.67	2.78	2.84
EI1	0.97	2.45	3.04	0.53	3.57	5.91	7.14	-	-	3.72	4.88	2.19	2.26
EI2	0.92	0.94	1.49	0.53	0.65	2.36	2.67	0.70	1.42	1.58	1.80	0.78	0.87
II1	1.09	0.57	1.22	0.52	3.57	4.08	5.31	-	-	3.29	4.28	0.79	1.03
II2	1.50	0.25	1.15	0.52	0.65	2.01	2.32	0.75	1.44	1.72	2.06	0.29	0.26
CW1	2.79	2.34	4.01	0.52	3.57	6.87	8.10	-	-	4.48	5.66	2.39	2.44
CWI2	2.79	0.93	2.61	0.52	0.65	3.47	3.78	0.55	1.29	2.72	3.02	0.75	0.76
CWI3	1.85	0.54	1.65	0.52	0.65	2.51	2.82	-	-	2.08	2.41	0.43	0.41

[a]A similarity between the results obtained by the proposed method and the default values given in EN ISO 14683 is not expected, because the floor sections in this standard have no web beam. However, the use of floor with beam is quite widespread in the earthquake regions. Sections marked "-" are not defined in the Standard at all. [b]Values calculated using the equation "$\sum A \cdot U + \sum \ell \cdot U_l$" for the sections with the lengths of walls and r.c. floor slab from outside corner equal to 0.80 m for 1 m section thickness. According to the 2D analysis results, 1D heat transfer starts within a distance much less than 0.80 m from the boundaries of the web beam. The results of calculations (not included in this paper) showed that the U_l value did not vary with the dimensions of the wall, slab or parapet. [c]Values calculated using the equation "$\sum A \cdot U + \sum \ell \cdot U_l$" for the sections with the lengths of walls and r.c. floor slab from inside corner equal to 1.00 m for 1 m section thickness. This value can be considered to be equivalent to L^{2D} used in EN 13789 and given in EN ISO 14683.[d] Amount of heat transmitted through the outer surface of the section (length of walls and floor slab measured from outside corner are 0.80 m) for 1 m section thickness. [e]Amount of heat transmitted through the outer surface of the section (length of walls and floor slab measured from inside corner are 1.00 m) for 1 m section thickness.

Table 4. Error analysis of the QuickField results.

For series A					For series B				
Total Q positive	Total Q negative	Sum with sign	Half of absolute sum	Sum with sign/half of absolute sum	Total Q positive	Total Q negative	Sum with sign	Half of absolute sum	Sum with sign/half of absolute sum
4.98	5.26	-0.28	5.12	-0.055	6.35	6.64	-0.29	6.50	-0.045
5.00	5.30	-0.30	5.15	-0.058	6.37	6.67	-0.30	6.52	-0.046
3.58	3.72	-0.14	3.65	-0.038	4.95	4.88	0.07	4.92	0.014
1.50	1.58	-0.08	1.54	-0.052	1.76	1.80	-0.04	1.78	-0.022
3.32	3.29	0.03	3.31	0.009	4.08	4.11	-0.03	4.10	-0.007
1.74	1.72	0.02	1.73	0.012	2.04	2.03	0.01	2.04	0.005
4.24	4.48	-0.24	4.36	-0.055	5.40	5.66	-0.26	5.53	-0.047
2.49	2.72	-0.23	2.61	-0.088	2.78	3.02	-0.24	2.90	-0.083
1.94	2.08	-0.14	2.01	-0.070	2.24	2.38	-0.14	2.31	-0.061

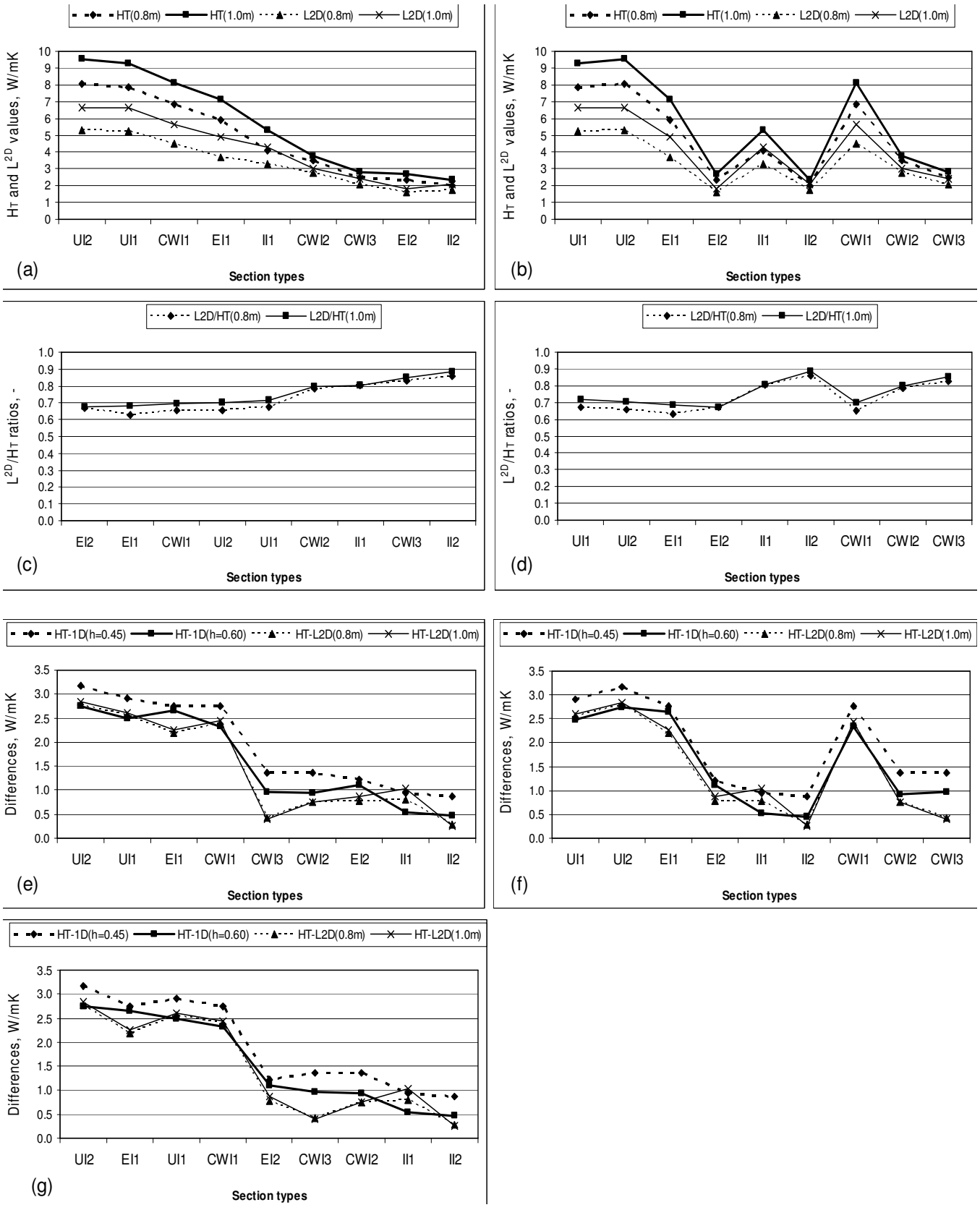

Figure 3. Comparison of the H_T (calculated by the proposed method) and L^{2D} values versus section types.

Table 5. Comparison of the H_T, L^{2D} and 1D values obtained by different methods for typical sections.

Section types	Results by 1D analysis				Results by the proposed method		Results by 2D analysis		Difference from 1D analysis results							
	§ h=0.45m		§§ h=0.60m		H_T[b]	H_T[c]	L^{2D} [d]	L^{2D} [e]	H_T[b] -1D		H_T[c] -1D		L^{2D} [d] -1D		L^{2D} [e] -1D	
									§	§§	§	§§	§	§§	§	§§
	W/(m·K)		W/(m·K)		W/(m·K)		W/(m·K)		W/(m·K)		W/(m·K)		W/(m·K)		W/(m·K)	
UI1	4.91	6.33	5.34	6.76	7.82	9.25	5.26	6.64	2.92	2.49	2.92	2.49	0.35	-0.08	0.31	-0.12
UI2	4.91	6.33	5.34	6.76	8.08	9.51	5.30	6.67	3.18	2.75	3.18	2.75	0.39	-0.04	0.34	-0.09
EI1	3.15	4.38	3.25	4.48	5.91	7.14	3.72	4.88	2.76	2.66	2.76	2.66	0.57	0.47	0.50	0.40
EI2	1.15	1.46	1.25	1.56	2.36	2.67	1.58	1.80	1.21	1.11	1.21	1.11	0.43	0.33	0.34	0.24
II1	3.14	4.37	3.55	4.78	4.08	5.31	3.29	4.28	0.94	0.53	0.94	0.53	0.15	-0.26	-0.09	-0.50
II2	1.14	1.45	1.55	1.86	2.01	2.32	1.72	2.06	0.87	0.46	0.87	0.46	0.58	0.17	0.61	0.20
CWI1	4.12	5.34	4.55	5.77	6.87	8.1	4.48	5.66	2.76	2.33	2.76	2.33	0.36	-0.07	0.32	-0.11
CWI2	2.12	2.42	2.55	2.85	3.47	3.78	2.72	3.02	1.36	0.93	1.36	0.93	0.60	0.17	0.60	0.17
CWI3	1.14	1.45	1.55	1.86	2.51	2.82	2.08	2.41	1.37	0.96	1.37	0.96	0.94	0.53	0.96	0.55

§: For left side of column ($\sum A \cdot U$) = $(0.8 \cdot 1 \cdot U_{wall})+(0.685 \cdot 1 \cdot U_{roof})+(0.45 \cdot 1 \cdot U_{TBbeam})$. §: For right side of column ($\sum A \cdot U$) = $(1 \cdot 1 \cdot U_{wall})+(1 \cdot 1 \cdot U_{roof})+(0.45 \cdot 1 \cdot U_{TBbeam})$. §§:For left side of column ($\sum A \cdot U$) = $(0.8 \cdot 1 \cdot U_{wall})+(0.685 \cdot 1 \cdot U_{roof})+(0.45 \cdot 1 \cdot U_{TBbeam})+(0.15 \cdot 1 \cdot U_{TBbeam(upper\ region)})$.§§:For right side of column($\sum A \cdot U$) = $(1 \cdot 1 \cdot U_{wall})+(1 \cdot 1 \cdot U_{roof})+(0.45 \cdot 1 \cdot U_{TBbeam})+(0.15 \cdot 1 \cdot U_{TBbeam(upper\ region)})$.In the calculation of $U_{TBbeam(upper\ region)}$, the thickness of the upper region of the beam was taken as the thicknesses of beam+insulation+inside plaster; the thermal conductance of this thickness was taken equal to that of reinforced concrete. [b c d e]See the footnotes in Table 3.

case of 2D heat flow.

If h is selected as 0.60 m (that is, upper region of the beam in contact with the indoor temperature), for the sections UI1, UI2, II1 and CWI1, L^{2D} values are smaller than 1D analysis results while for the other sections, the L^{2D} values are higher but close to 1D analysis results (Table 5). These are not reliable. If h is selected as 0.45 m (that is, upper region of the beam neglected), L^{2D}-1D values are positive for almost all sections, and between about 0.30 to 1.00 W/(m·K) (Table 5 and Figure 4). But the order of the sections is not significant from the point of view of 2D heat flow trend. On the contrary, the H_T values thus obtained are generally quite higher than those obtained by the 1D analysis. The differences (varying between 0.40 and 3.00 W/(m·K)) in monotonously decreasing order are UI2, EI1, UI1, CWI1, EI2, CWI2, CWI3, II1, II2 when h is selected as 0.60 m, whereas UI2, UI1, EI1, CWI1, CWI3, CWI2, EI2, II1, II2 when h is selected as 0.45 m (Figure 3c and 3d). This order is almost equivalent to the order of effectiveness of 2D heat flow. UI2, UI1, EI1, CWI1 have higher difference (2.50 to 3.00 W/(m·K)), and heat flow vectors are upwards almost throughout the whole beam section (Figure 2). CWI3, CWI2, EI2, II1, II2 with much lower differences (0.5 to 1.0 W/(m·K)), have roof insulation and/or dominant 1D heat flow.

It is worth noting that the curve of the difference H_T-L^{2D} is very similar to the H_T-1D curve (Figure 3c, 3d and 3g).

In Figure 5, the values L^{2D}-1D and H_T-1D are shown together with the ratios of (L^{2D}-1D)/L^{2D} and (H_T-1D)/H_T. The curve (L^{2D}-1D) is almost a horizontal line not indicating any significant distinction between thermal properties of the sections (i.e., existence and place of insulation). However, the curve of (H_T-1D), increasing continuously and having a threshold, represents the effectiveness of 2D heat flows in the sections (Figures 2 and 5). The ratios of (H_T-1D)/H_T are generally high (about 17-50%). All values are above 30% except II1 section for which 1D heat flow is quite dominant. On the contrary, the values of (L^{2D}-1D)/L^{2D} exhibit very large variation (between -5 and +40%) with no systematic and significant mean. It is obvious that the quantities (H_T) being harmonized with the 2D heat flow appearance or trend (Figure 2) reflect values relatively closer to the real ones.

H_T values are calculated again by the proposed method, different from Equation 7, by using the

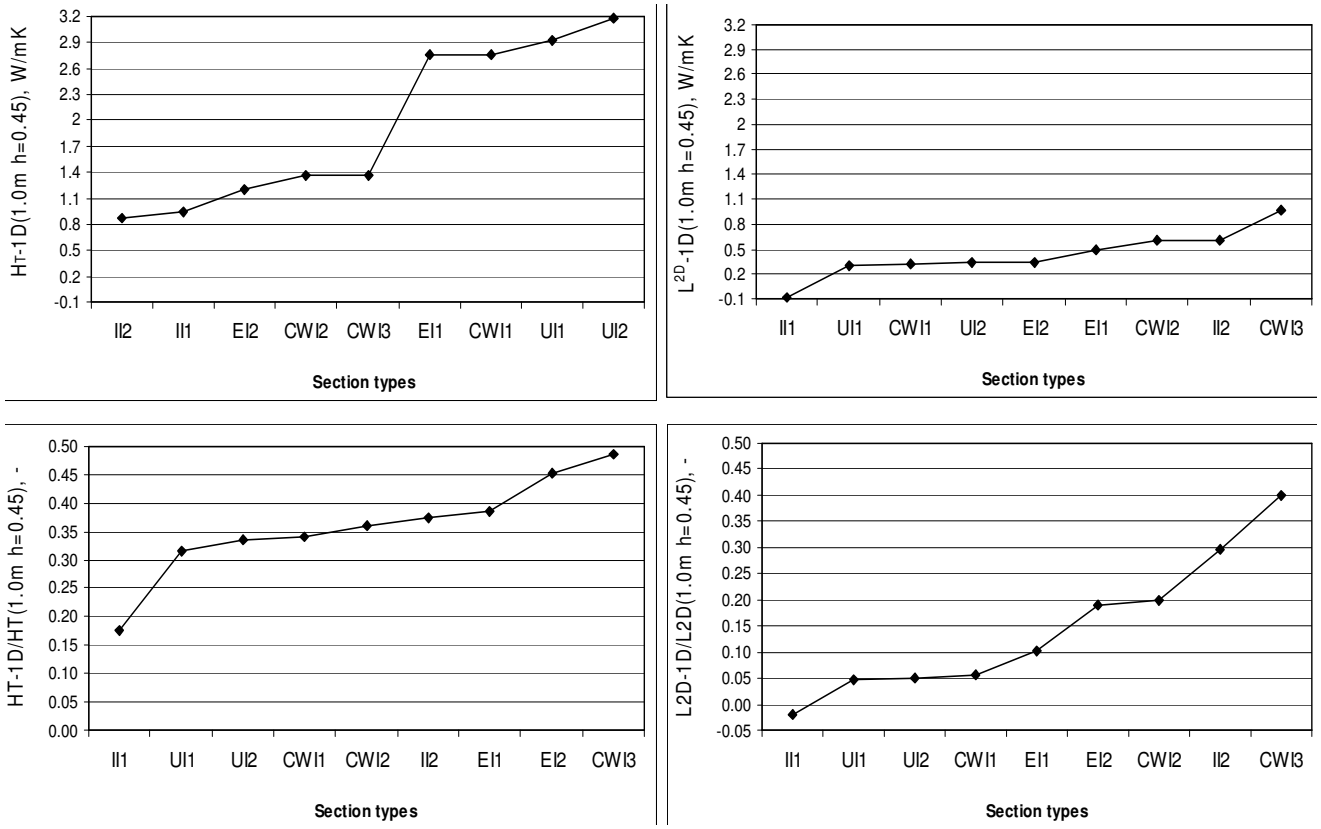

Figure 4. Comparison of the H_T and L^{2D} values with the 1D analysis results versus section types.

average volume heat flux density of the beam as a whole, without dividing the beam into regions. The H_T values thus obtained, the L^{2D} values and their differences are shown in Table 6 and Figure 4. In this case, H_T and L^{2D} values are relatively close to each other, indicating that the large difference between the H_T and L^{2D} values, appearing in the results of the previous calculations, were caused by thermal interactions occurring inside the beam (that is, the thermal bridge).

These indicate that L^{2D} values described in EN 10211-1, are not sensitive enough to the 2D heat flows for the sections of roof with parapet. The effects of heat flow from the beam to the parapet and the interaction through the beam section are not apparent in the L^{2D} values.

H_T values obtained by the proposed model with Equation (7) are in harmony with the results obtained by 2D analysis for floors (Dilmac et al., 2007). In these sections, the outgoing heat flows through the beam are dominantly in the x direction, (Dilmac et al., 2007). But for roofs, heat flow vectors are generally upwards, almost throughout the whole beam for some sections, and corner effect occurs.

On the other hand, it is interesting to note that the differences are significant between Series A and B for roofs unlike floors. Hence, the length of 1.00 m from the thermal bridge is needed for the wall and the slab from the beam intersection surface adjacent to roofs, as required in EN 10211.

Conclusions

In this paper, a method is proposed for the calculation of parameters cited in ISO 9164 for roof-wall intersections. H_T values obtained by the proposed method and calculated to be equivalent to the L^{2D} values for typical roof sections with web beams are compared with the L^{2D} values obtained by the methods given in EN 832, EN 13789, EN ISO 14683, and 2D analysis.

The numerical values show that the H_T values obtained by the proposed method for roofs are quite different from the L^{2D} values obtained by the EN ISO 14683 and 2D analysis performed using the QuickField program. Generally, the results obtained by the EN ISO 14683 method are less than those of the others as expected, because the sections in the standard have no web beams, and, therefore, the effects of thermal bridges are less pronounced than the others.

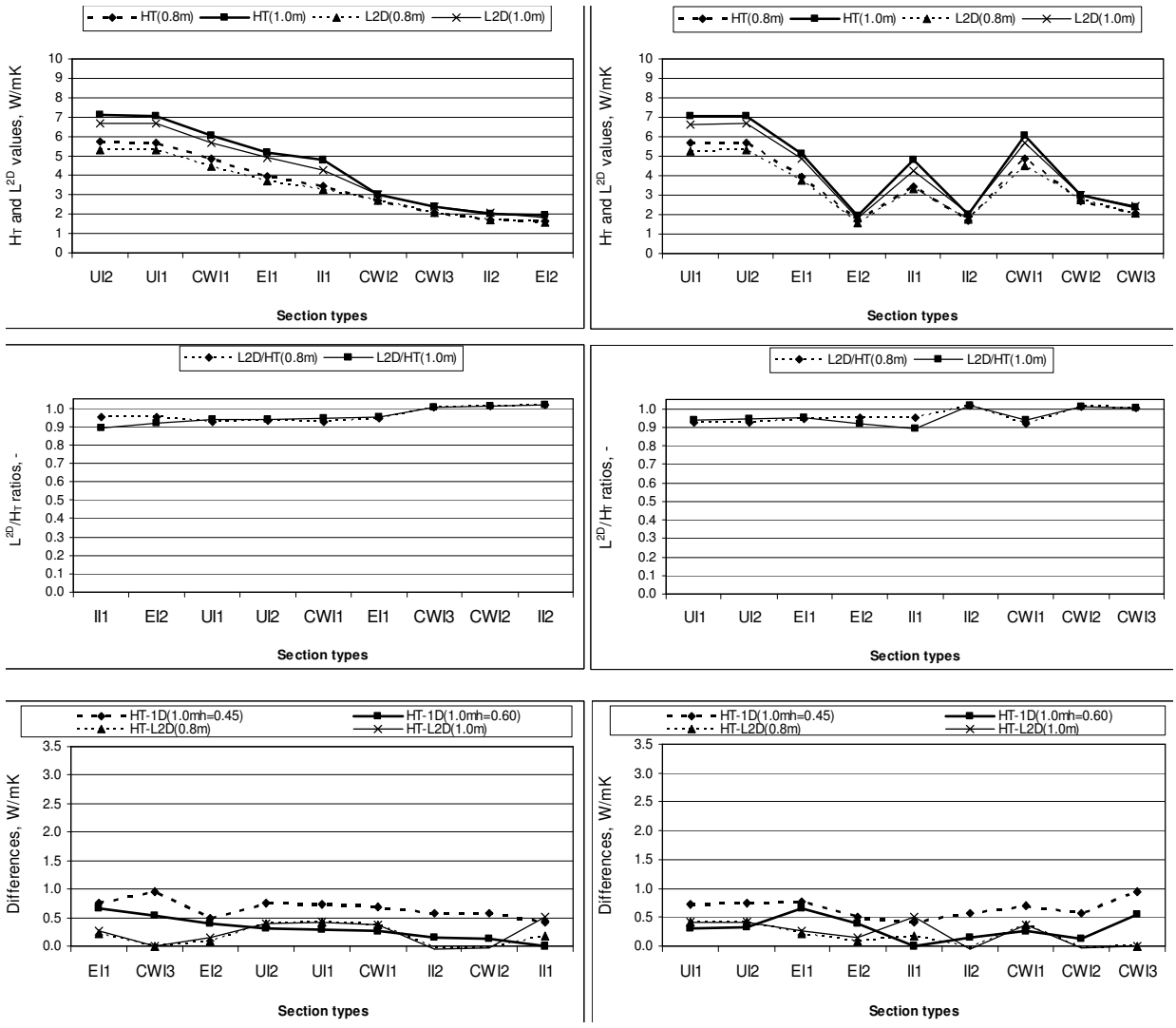

Figure 5. H_T calculated by the proposed method but using average volume heat flux density and L^{2D} values versus section types.

It is worth noting that the proposed method always gives significantly higher (H_T) values than (L^{2D}). As expected, H_T and L^{2D} values get smaller and come closer together for the roofs with insulation (Figures 2, 3a and d). These two quantities are getting closer at II2, EI2, CWI3, CWI2 and II1 sections in which 2D heat flow is less effective throughout the beam section, and/or the lengths of the heat flow vectors are smaller than those of the others. The higher differences between the H_T and L^{2D} values are seen at EI1, CWI1, UI1, and UI2 sections in which there is no roof insulation, and the heat flow throughout the beam section is clearly 2D.

The ratios (L^{2D}/ H_T) of external insulation with and without roof insulation (EI1 and EI2), uninsulated sections (UI1 and UI2) and cavity wall insulation without roof insulation (CWI1) are about 70% while those of CWI2, CWI3, II1 and II2 are higher up to about 90% (Figure 3b and 3f).

According to the L^{2D} analyses results, the sections arranged in the order of decreasing L^{2D} and H_T values caused by thermal bridge of roof-wall intersections are shown in Table 7. The order of the sections by the 2D analysis and the proposed method are similar except the last two lines (the reversal of positions of the II2 and the EI2 sections).

In calculation of H_T by the proposed method, q_y is determined by summing the absolute values of q_y of each region of beam (Equation 7). Hence, this q_y defines the heat transfers (thermal interaction) in the beam and it is more sensitive to the 2D heat flow throughout the beam caused by insulation type than L^{2D}. To assess which of the two is more accurate and closer to the real value,

Table 6. Comparison of the parameters calculated by the proposed method using average volume heat flux density with those calculated by the 2D analysis.

Section types	q_y [a]	ξ [a]	H_T [a]	q_y [b]	ξ [b]	H_T [b]	L^{2D} [c]	L^{2D} [d]	H_T [a]-L^{2D} [c]	H_T [b]-L^{2D} [d]
	W/m^2	W/(m·K)	W/(m·K)	W/m^2	W/(m·K)	W/(m·K)	W/(m·K)	W/(m·K)	W/(m·K)	W/(m·K)
UI1	1.05	0.36	5.68	1.05	0.36	7.06	5.26	6.64	0.42	0.42
UI2	1.13	0.38	5.71	1.12	0.38	7.08	5.30	6.67	0.41	0.41
EI1	1.34	0.50	3.95	1.36	0.51	5.14	3.72	4.88	0.23	0.26
EI2	0.64	0.24	1.66	0.65	0.24	1.96	1.58	1.80	0.08	0.16
II1	0.27	0.10	3.46	0.27	0.10	4.79	3.29	4.28	0.17	0.51
II2	-0.11	-0.04	1.69	-0.11	-0.04	2.02	1.72	2.06	-0.03	-0.04
CWI1	0.96	0.33	4.86	0.96	0.33	6.04	4.48	5.66	0.38	0.38
CWI2	0.46	0.16	2.69	0.46	0.16	2.99	2.72	3.02	-0.03	-0.03
CWI3	0.33	0.13	2.07	0.33	0.13	2.40	2.08	2.41	-0.01	-0.01

[a] and [c] are for series A, [b] and [d] are for Series B. H_T values are calculated for 1 m section thicknesses.

Table 7. Comparison of the results.

2D analysis (QuickField 5.0)			H_T (proposed method)			L^{2D} (EN ISO 14683)		
Section	L^{2D} W/(m·K)	100·L^{2D}/ $L_{2D\ UI2}$(%)	Section	H_T W/(m·K)	100·H_T/$H_{T\ UI2}$ (%)	Section	L^{2D} W/(m·K)	100·L^{2D}/ $L_{2D\ II2}$ (%)
UI2	6.67	100	UI2	9.51	100	II2	1.44	100
UI1	6.64	100	UI1	9.25	97	EI2	1.42	99
CWI1	5.66	85	CWI1	8.10	85	CWI2	1.29	90
EI1	4.88	73	EI1	7.14	75			
II1	4.28	64	II1	5.31	56			
CWI2	3.02	45	CWI2	(3.78	40			
CWI3	2.41	36	CWI3	2.82	30			
II2	2.06	31	EI2	2.67	28			
EI2	1.80	27	II2	2.32	24			

each value is compared with the corresponding value calculated by 1D analysis. The differences, that is, L^{2D}-1D values were sometimes negative, and the L^{2D}-1D values order of the sections is not in significant compliance with 2D heat flow appearance (Figure 5). On the contrary, H_T values are generally quite higher than 1D analysis results. The order is approximately equivalent to the order of effectiveness of 2D heat flow. The curve (L^{2D}-1D) is almost a horizontal line not reflecting the thermal properties of the sections (i.e., state and place of insulation). But the (H_T-1D) curve, increasing continuously with a jump, represents the effectiveness of 2D heat flows in the sections (Figures 3 and 5). It is worth noting that the H_T-L^{2D} curve is very similar to the H_T-1D curve (Figure 3c, 3d and 3g). The (H_T-1D)/H_T ratios are generally high (about 17 to 50%). All values are above 30% except at Section II1 for which 1D heat flow is quite dominant. On the contrary, the (L^{2D}-1D)/L^{2D} values exhibit very large variation (between -5 and +40%) with no systematic and significant mean. It is obvious that the H_T values, consistent with the apparent 2D heat flow, are relatively close to real value.

H_T values are calculated again by the proposed method, but differently from the Equation 7, by using the average volume heat flux density of the beam as a whole, without dividing the beam into regions. So the interaction inside the beam is neglected. In this case, H_T and L^{2D} values are relatively close to each other, indicating that the large difference between the H_T and L^{2D} values, appearing in the results of the previous calculations, were caused by the thermal interactions occurring inside the beam, i.e., the thermal bridge.

These indicate that L^{2D} values described in EN 10211-1, are not sensitive enough to the 2D heat flows for the sections of roof with parapet. The effects of heat flow from the beam to the parapet and the interaction through the beam section are not apparent in the L^{2D} values.

H_T values obtained by the proposed model with Equation 7 are in harmony with the results obtained by 2D analysis for floors (Dilmac et al., 2007). In these

sections, the outgoing heat flows through the beam are dominantly in the *x* direction, (Dilmac et al., 2007). But for roofs, heat flow vectors are generally upwards, almost throughout the whole beam for some sections, and corner effect occurs.

On the other hand, it is interesting to note that the differences are significant between Series A and B for roofs unlike floors. Hence, the length of 1.00 m for the walls and the slab from the beam intersection surface as required in EN 10211 is important for roofs.

ACKNOWLEDGEMENT

This work was funded by the Scientific and Technological Research Council of Turkey (TUBITAK) under project no. ICTAG -I242.

REFERENCES

Al-Anzi A, Krarti M (2004). Local/global analysis of transient heat transfer from building foundations. Build. Environ., 39: 495-504.

Al-Sanea SA (2003). Finite-volume thermal analysis of building roofs under two-dimensional periodic conditions. Build. Environ., 38: 1039-1049.

Anon EN 832 (2000). Thermal Performance of Buildings, Calculation of Energy Use for Heating, Residential Buildings, European Committee for Standardization, Brussels.

Anon EN ISO 10211-1 (1996). Thermal bridges in building construction-Heat flows and surface temperatures -Part 1: General calculation methods, European Committee for Standardization, Brussels.

Anon EN ISO 13789 (1999). Thermal performance of buildings-Transmission heat loss coefficient-Calculation methods, European Committee for Standardization, Brussels.

Anon ISO 14683 (1999). Thermal bridges in building construction - Linear thermal transmittance-Simplified methods and default values, the International Organization for Standardization, Geneva.

Anon ISO 9164 (1989). Thermal Insulation-Calculation of space Heating Requirements for Residential Buildings, International Organisation for Standards, Geneva.

Brown WP, Wilson AG (1963). Thermal Bridge in Buildings. National Research Council Canada. Institute for Research in Construction. http://irc.nrc.cnrc.gc.ca/cbd/cbd044e.html (originally published).

Deque F, Ollivier F, Roux JJ (2001). Effect of 2^D modelling of thermal bridges on the energy performance of buildings Numerical application on the Matisse apartment. Ener. Build., 33: 583-587.

Dilmac S, Cihan MT, Guner A (2004). Teras catilarin enerji verimliliklerinin karsılastirilmasi. Dizayn Konstruksiyon. 226: 68-77.

Dilmac S, Guner A, Senkal F, Kartal S (2007). Simple method for calculation of heat loss through floor/beam-wall intersections according to ISO 9164. Ener. Convers., Manage., 48: 826-835.

Fukuyo K (2003). Heat flow visualization for thermal bridge problems. Int. J. Refr., 26: 614-617.

Hassid S (1989). Thermal bridges in homogeneous walls: A simplified approach. Build. Environ., 24: 259-264.

Hassid S (1990). Thermal bridges across multilayer walls: An integral approach. Build. Environ., 25: 143-150.

Kosny J, Kossecka E (2002). Multi-dimensional heat transfer through complex building envelope assemblies in hourly energy simulation programs. Ener. Build., 34: 445-454.

Larbi AB (2005). Statistical modelling of heat transfer for thermal bridges of buildings. Energy and Buildings. 37: 945-951.

Lefebvre G (1997). Modal-based simulation of thermal behaviour of a building: the $m2^m$ software. Ener. Build., 25: 19-30.

Malas MV, Letherman KM (1992). Heat transfer analysis of diaphragm walls with high thermal insulation. Build. Environ., 27: 57-61.

Mao G, Johannesson G (1997). Dynamic calculation of thermal bridges. Energy and Buildings. 26: 233-240.

Matrosov YA, Butovsky IN (1989). USSR experience in thermal design of building envelopes with improved thermal properties. Ener. Build., 14: 31-41.

Salgon JJ, Neveu A (1987). Application of model analysis to modelling of thermal bridges in buildings. Energy and Buildings. 10: 109-120.

Van Schijindel AWM (2003). Modelling and solving building physics problems with FemLab. Build. Environ., 38: 319-327.

Yahia AA, Del Barrio EP (1999). Thermal systems modelling via singular value decomposition: direct and modular approach. Appl. Math. Mod. 23: 47-468.

Zhai Z, Chen Q, Haves P, Klems JH (2002). On approaches to couple energy simulation and computational fluid dynamic programs. Build. Environ., 37: 857-864.

NOMENCLATURE

A	Area of exposed facet	m^2
b	Width of the thermal bridge	m
d	Thickness	m
H	Specific heat loss	W/K
H_U	Transmission heat loss coefficient between heated space and external environments via unheated spaces	W/K
h	Height	m
ℓ	Length of thermal bridge	
L^{2D}	Thermal coupling coefficient obtained from a two-dimensional calculation,	W/(m·K)
L^{3D}	Thermal coupling coefficient obtained from a three-dimensional calculation	(W/K)
L_D	Direct coupling coefficient between the heated space and exterior through building envelope	W/K
L_s	Steady state ground heat loss coefficient	W/K
Q	Space heating requirement	J
q	Heat flux density	W/m^2
T	Temperature	K, °C
t	Time	s
U	Thermal transmittance of exposed fabric	$W/(m^2 \cdot K)$
U_ℓ	Linear thermal transmittance of thermal bridge	W/(m·K)
α	Surface heat transfer coefficient	$W/(m^2 \cdot K)$
η	Utilization factor for gains	-
$\Lambda=\sum d/\lambda$	Thermal transmittance from surface to surface of exposed fabric	$W/(m^2 \cdot K)$
λ	Thermal conductivity	W/(m·K)
ξ	Factor characteristic of the thermal bridge	W/(m·K)
φ	Average gains over month, angle	W, °
χ	Point thermal transmittance of point thermal bridge	W/K
ψ	Linear thermal transmittance of thermal bridge	W/(m·K)

Indices

c	Concrete
e	Environment, equivalent
h	Hour
i	Indoor
ins.	Insulation
ip	Indoor plaster
is	Indoor surface
ℓ	Lower
m	Month, middle, mean
oi	Overall internal
op	Outdoor plaster
os	Outdoor surface
pos	Sum is carried out for positive values
q_x	Heat flux density in the “x” direction, obtained from 2D analysis
s	Solar
T	Transmission
TB	Thermal Bridge
u	Upper
V	Ventilation
x	“x” direction
y	“y” direction